Hindawi
Advances in Meteorology
Volume 2019, Article ID 4328151, 15 pages
https://doi.org/10.1155/2019/4328151

Research Article

Simulation of Threshold UV Exposure Time for Vitamin D Synthesis in South Korea

Sang Seo Park,[1] Yun Gon Lee,[2] Migyoung Kim,[2] Jaemin Kim,[2] Ja-Ho Koo,[3] Chang Ki Kim,[4] Junshik Um,[5] and Jongmin Yoon[6]

[1]*School of Earth and Environmental Sciences, Seoul National University, Seoul, Republic of Korea*
[2]*Department of Atmospheric Sciences, Chungnam National University, Daejeon, Republic of Korea*
[3]*Department of Atmospheric Sciences, Yonsei University, Seoul, Republic of Korea*
[4]*New and Renewable Energy Resource Center, Korea Institute of Energy Research, Daejeon, Republic of Korea*
[5]*Department of Atmospheric Sciences, Pusan National University, Busan, Republic of Korea*
[6]*National Institute of Environmental Research, Incheon, Republic of Korea*

Correspondence should be addressed to Yun Gon Lee; yungonlee@gmail.com

Received 8 August 2018; Revised 5 December 2018; Accepted 24 December 2018; Published 27 January 2019

Academic Editor: Harry D. Kambezidis

The threshold exposure time for synthesis of vitamin D was simulated by using a radiative transfer model considering variations in total ozone, cloud, and surface conditions. The prediction of total ozone took the form of an empirical linear regression with the variables of meteorological parameters in the upper troposphere and lower stratosphere and the climatology value of total ozone. Additionally, to consider cloud extinction after the estimation of clear-sky UV radiation using a radiative transfer model simulation, a cloud modification factor was applied. The UV irradiance was estimated at one-hour intervals, and then, to improve the temporal resolution of the exposure time simulation, it was interpolated to a one-minute resolution. Exposure times from the simulation clearly followed seasonal and diurnal cycles. However, upon comparison with observations, biases with large variations were found, and the discrepancy in the exposure time between the observations and simulations was higher in low UV irradiance conditions. The large deviations in the prediction errors for total ozone and the simplified assumption for the cloud modification factor contributed to the large deviations in exposure time differences between the model estimation and observations. To improve the accuracy of the simulated exposure time, improved predictions of total ozone with a more detailed cloud treatment will be essential.

1. Introduction

Increases in surface UV irradiance resulting from stratospheric ozone depletion have had harmful effects on human health by inducing skin damage [1, 2]. To assess the health risks from UV, erythemally weighted UV (UV_{Ery}) or the UV index (UVI; defined by UV_{Ery} in Wm^{-2} divided by 25 mWm^{-2}) has been developed using a weighted function related to the occurrence of skin erythema [3, 4, 5, 6]. UV_{Ery} irradiance (or the UVI) generally varies with atmospheric conditions that include the quantity of ozone, which is an important factor in its accurate estimation. The widely used action spectrum for the erythemal dose is that of the Commission International on Illumination (CIE) [5]. Because prolonged exposure to UV_{Ery} leads to harmful erythemal dosing, UV_{Ery} observation networks have focused primarily on UV-B (ranges from 280 to 315 nm) measurements, with some consideration of UV-A (ranges from 315 to 400 nm) measurements [7]. In addition to its adverse effects, UV radiation has several beneficial effects on human health, such as perceived improved appearance, enhanced mood through endorphin release, and a reduction of blood pressure [8, 9]. The synthesis of vitamin D in the skin can be used as a representation of the beneficial effects of UV exposure [10–14].

The idea of adequate UV exposure time is defined as the UV exposure that balances the risks and benefits of UV

exposure to the skin [15]. The wavelengths of UV radiation for synthesizing vitamin D fall primarily in the UV-B and part of the short UV-A bands (shorter than 330 nm) [16, 17], which is similar to the spectral weight of UV_{Ery}. However, the effective range for the action spectrum is shorter than the CIE erythemal action spectrum [15, 18, 19, 20]. From previous studies, the optimized exposure time for vitamin D synthesis is normally shorter than the time required to cause erythema [15]. Therefore, the exposure time to solar UV radiation that results in sufficient vitamin D synthesis without damaging the skin can be determined.

The threshold value of exposure time is used to minimize the risk of erythemal dosing and to secure vitamin D synthesis. Therefore, exposure time calculations require accurate calculations of UV_{Ery} and the UV irradiance spectra weighted by the action spectrum of vitamin D synthesis (UV_{VitD} hereafter). The latter is related to the production of 25-hydroxy vitamin D. However, the solar UV irradiance at the surface changes diurnally and seasonally due to the geometrical changes in solar position. For example, the UV_{Ery} irradiance in the midlatitudes is similar to that in the tropics during the summer, but it is lowered by approximately 90% during the winter [15, 21] due to the large seasonal variation in the solar zenith angle. In addition to the solar position, atmospheric factors such as ozone concentrations [22, 23], aerosol [22, 23, 24], and cloud coverage [25, 26] diminish surface UV irradiance. Comprehensively, diminishing surface UV irradiance by the atmospheric conditions caused the "vitamin D winter" effects, which is a season with insufficient vitamin D synthesis by UV irradiance [27, 28].

Focusing on studies that have calculated exposure time, the regional distribution of the levels of threshold of UV exposure for vitamin D synthesis have been determined by using the statistical relationship between UV_{VitD} and several variables, such as global solar irradiance, total ozone, and dew point temperature [27, 29]. In addition, Miyauchi et al. [30] noted that the UV_{VitD} and exposure time calculations have also been developed based on a radiative simulation combined with various elements of observation data. The latter considers the season, time, and spatial variation of atmospheric conditions.

In South Korea, the forecast system of daily maximum UV_{Ery} is developed based on a statistical linear regression model for total ozone that uses long-term satellite datasets from the Total Ozone Mapping Spectrometer (TOMS) and the Ozone Monitoring Instrument (OMI) [31], which is similar to the UV_{Ery} simulation systems used in other regions [24, 32, 33, 34, 35, 36, 37]. However, the estimation of UV_{VitD} and exposure time simulations for it, which accounts for atmospheric conditions with high temporal and spatial resolution, have not yet been reported. This study provides a simulated exposure time for vitamin D synthesis based on an improved UV calculation. During the UV calculation, we also considered to the information of total ozone prediction from statistical approach and cloud forecast from the model simulation in South Korea as shown in Section 2. Finally, Section 3 describes the simulation results of exposure time and comparison in several observation sites.

2. Exposure Time Calculation Based on the Simulation

Figure 1 shows a flow chart of the simulation of UV_{VitD} exposure time. The simulated UV_{VitD} is based on the calculation method for daily representative UVI, defined as the noon-time value, over Korea [31]. In several previous studies, for clear-sky UV calculations using radiative transfer models (RTMs), total column ozone has been predicted based on results from empirical linear regression models [31, 32, 38] or chemical transport models [39]. In this study, the simulation consists of a total ozone model based on empirical regression. As described in Section 2.1, the total ozone prediction is daily representative total ozone forecast on the next day with using parameters from the results of numerical weather predictions. A cloud modification factor is applied to the UV irradiance results to calculate the UVI and UV_{VitD} (Section 2.2). Finally, the method of calculation of the UV exposure time is shown in Section 2.3.

2.1. Total Ozone Prediction. The quantity of total ozone in the midlatitude region depends on the activity of the Brewer–Dobson circulation and stratosphere–troposphere exchange in the Arctic [40, 41]. In South Korea, Park et al. [42] have reported on the total ozone, as well as the annual, seasonal, and day-to-day variation of total ozone. Using a 25-year set of ground- and satellite-based observational data, the interannual variation was found to be less than 20 Dobson Unit (DU). The seasonal variation ranged from 51 to 106 DU, which corresponds to approximately 17%–30% of the total ozone. This large temporal variation is the result of solar activity and the natural oscillations that affect stratospheric ozone. However, according to an analysis of the daily representative total ozone dataset [42], the day-to-day ozone variation, which is defined as the relative difference in total ozone between a given day and the day prior, ranged from −30.3% to 38.6%, with a mean absolute difference of 5.2~5.7%. In addition, variation in column amount of ozone in the stratosphere, which is known to be less variable than that in the troposphere, has been estimated to be 13.4 DU for a standard deviation from ozonesonde observations over the Korean Peninsula [41]. This short-term temporal variation is caused mainly by the heterogeneity of the distribution of stratospheric ozone and its dynamic transport. Based on these observations, total ozone variations on a daily scale must be considered when estimating surface UV irradiance.

The total ozone dataset was compiled from observations from the Dobson spectrophotometer at Yonsei University, Seoul (WMO/GO3OS Station No. 252, location: 37.57°N, 126.95°E, 84 m above sea level). The quality of the Dobson data was validated using a dataset from the Brewer spectrophotometer at Pohang [41], overpass data from TOMS [41, 43, 44, 45], and data from OMI [41, 46, 47]. From the intercomparison studies, the total ozone from the other instruments agreed within 2% with that from the Dobson spectrophotometer.

The atmospheric factors, daily total ozone data, and its climatology were used to develop the daily total ozone

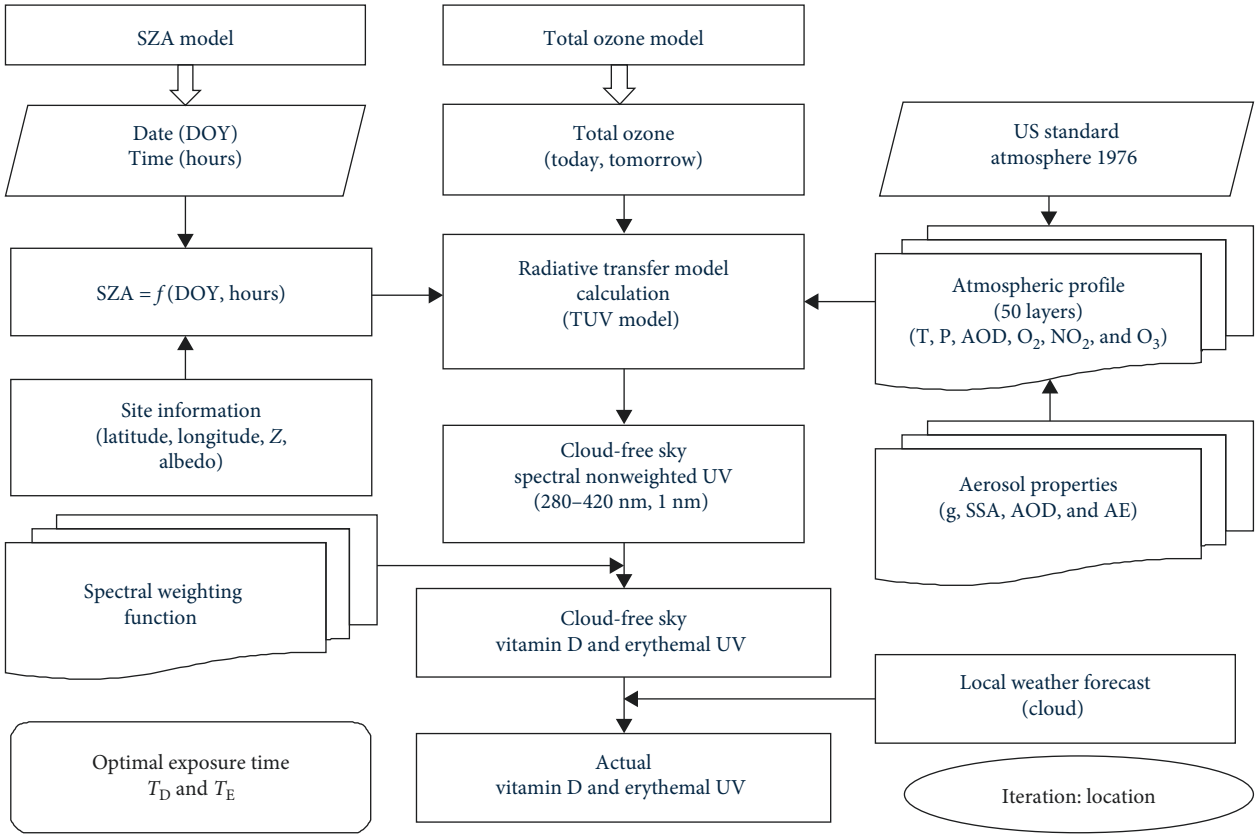

Figure 1: Flow chart of forecast system of exposure time for vitamin D synthesis.

prediction on the next day $(D+1)$ by using the linear regression method. The training period for the linear regression was 44 months, from May 2011 to December 2014. To account for the long-term variations of total ozone considering seasonal and annual scales, a 30-year dataset from 1985 to 2014 was used as the climatological total ozone dataset for total ozone prediction. Because total ozone variations on a daily scale are strongly related to atmospheric conditions in the stratosphere and upper troposphere, we selected u-wind, v-wind, temperature, and geopotential height from 100 to 300 hPa at the site of the Dobson spectrophotometer as variables for the empirical regression. These meteorological variables were derived from data from the regional data assimilation and prediction system (RDAPS) model of the unified model (UM) from the KMA, which has a horizontal resolution of 12 km × 12 km. Using forward stepwise selection, significant meteorological variables were identified for use in the prediction of daily total ozone and the empirical regression formula is shown below:

$$\begin{aligned} c(D+1) = {} & 0.437 \times c + 0.479 \times c_c + 0.293 \times v(100\,\text{hPa}) \\ & - 0.293 \times u(150\,\text{hPa}) - 0.018 \times h(100\,\text{hPa}) + 1.192 \\ & \times T(250\,\text{hPa}) + 2.268 \times T(100\,\text{hPa}) - 413.488, \end{aligned} \tag{1}$$

where $c(D+1)$ is the predicted total ozone amount on the next day $(D+1)$; c and c_c are the observed total ozone amount and climatology of total ozone using the 30-year dataset (period: 1985–2014) for a specific day, respectively; and u, v, T, and h are u-wind, v-wind, temperature, and geopotential height at a specified pressure, respectively. Based on the regression model for total ozone prediction, as shown in Figure 2, during the period from May 2011 to December 2014, the differences in total ozone between observed and estimated have a mean of 0.3% with a root mean squared difference of 5% (17.6 DU).

2.2. Cloud Modification Factor. Clouds, including their quantity, type, and optical properties, vary in time and space in the real atmosphere, and the UV attenuation by the cloud has large variability due to the variation of cloud properties. To estimate the radiative effect of cloud, most methods used to the cloud modification factor (CMF) as defined by the ratio between actual irradiance and clear-sky irradiance [25, 48, 49, 50]. Most of CMF value is less than 1.0, which means the existence of cloud diminishes the surface UV irradiance [51, 52]. Otherwise, several previous studies showed that observed UV-B irradiance was significantly enhanced by the cloud [53, 54, 55], and the cloud effect for UV-B has spectral dependence [56, 57, 58]. The CMF value is basically related to the cloud cover (cloudiness) with empirical approaches from the observation [59]. In addition, the CMF value is also dependent on the cloud altitude, cloud types, cloud thickness, and solar zenith

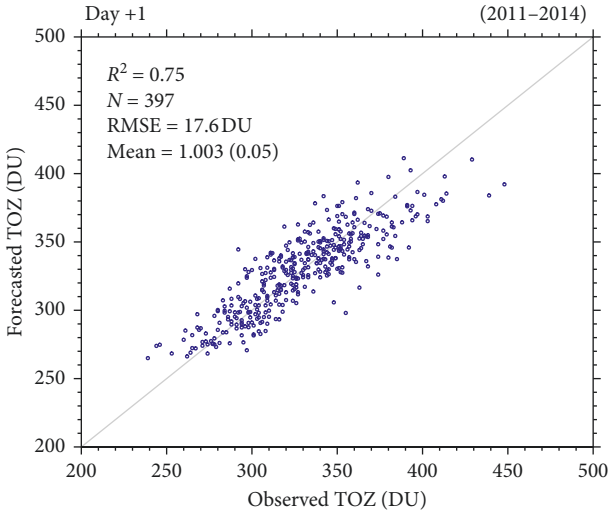

Figure 2: Relation between the observed and predicted total ozone amount for $(D+1)$ value.

angle to consider the geometrical dependence of UV scattering [55, 60, 61, 62].

The UV irradiances calculated from the RTM were basically conducted under cloud-free conditions. To consider the extinction by cloud, the parameters for cloud (e.g., cloud optical depth, phase function, and cloud vertical distribution) could be used as an input of RTM simulation. However, the KMA provided the predicted cloud amounts based on the tenth-scale with high spatial resolution. Because the RTM is a one-dimensional model that does not account for spatial variation, its irradiance includes uncertainties related to the cloud extinction from the cloudiness value. Although the cloud optical depth can be used as an input to the RTM, it is difficult to directly convert from cloudiness to cloud optical depth. In this study, the CMF value is used to consider the extinction of cloud in the simulation, and the CMF is the spectrally independent value. The CMF is simply defined by the cloud amount introduced from Lee et al. [31]:

$$\mathrm{CMF} = -0.0089 \times f^2 + 0.04 \times f + 0.940, \quad (2)$$

where f is the modeled cloud amount in tenths (fractional cover multiplied by ten). From the previous study in South Korea, the quantitative value of spectral difference of CMF in 320~360 nm is up to 0.05 [63], which is equivalent to the CMF error by cloud amount error of 1.25.

Because the meteorological forecast model provides cloud amount with 3-hour intervals, the CMF values also have a 3-hour resolution. Although the model calculates the UV irradiance with high temporal resolution, the CMF values changes every three hours. In the UV irradiance model, the CMF for a cloud amount of 0–2 is defined to be 0.984, which is considered as the maximum value and occurs under low-cloud conditions. The CMF from observation was estimated up to 0.95 for solar zenith angle of 40~70° [63]. The calculated cloud amount values have been grouped into five cloud-coverage categories at intervals of approximately 2-3.

2.3. Exposure Time Calculation. The clear-sky UV irradiance was calculated using an RTM for the tropospheric ultraviolet and visible (TUV) [64, 65]. The TUV model uses a radiative transfer method for shortwave irradiance calculations based on the two streams or discrete ordinates with multistreams. Atmospheric conditions were based on the standard atmosphere of the US including vertical profiles of molecular composition, temperature, and pressure discretized into several vertical layers. In addition to the input variables required for the RTMs used for the UV calculations, we also considered the aerosol conditions. An aerosol optical depth (AOD) of 0.5, single scattering albedo (SSA) of 0.95, and asymmetry factor (ASY) of 0.75 at 340 nm were used, which are similar to the observed optical parameters of aerosols in Seoul [66]. The SSA and ASY were assumed to be constant within the UV range, while the AOD had a spectral dependence with an angstrom exponent of 1.0.

The surface albedo was used as an input parameter to represent the surface properties. The land-cover type climate modeling grid (CMG) product (MCD12C1) was used to define the surface conditions. The MCD12C1 provides high spatial resolution (0.05°) coverage of the dominant land-cover types along with an "urban" surface type. Based on the "urban type" from MCD12C1, the urban index was defined as the total number of grid point for "urban type" in 4 grid points near a specific site. Using the urban index, the surface type was categorized into urban and suburban regions. The surface albedo ranged from 0.02 over grass [67] to 0.12 over concrete surfaces [68], near regions of industrial and human activity. Based on the previous studies, the urban index can be directly converted to the surface albedo using the following formula:

$$\mathrm{SUF} = 0.020 + 0.025 \times \mathrm{UI}, \quad (3)$$

where SUF and UI are the surface albedo and urban index (ranges from 0 to 4), respectively. The reference year for the surface types is 2012, which is the most current dataset for MCD12C1. The TUV calculates the UV irradiance from 280 to 420 nm with a 1 nm resolution. The forecasted clear-sky UV irradiance, UVI, and $\mathrm{UV_{VitD}}$ were estimated at one-hour intervals during the daytime.

The exposure time calculation for vitamin D synthesis is based on McKenzie et al. [15] and summarized below. Accordingly, the dose of vitamin D (DUVI) can be expressed as

$$\mathrm{DUVI} = \frac{[k \times \mathrm{UVI} \times \mathrm{R_{UV}} \times \mathrm{TD} \times \alpha]}{[\mathrm{MEDF} \times \mathrm{SPF}]}, \quad (4)$$

where R_{UV} is the ratio of $\mathrm{UV_{Ery}}$ to $\mathrm{UV_{VitD}}$ as a function of the solar zenith angle and total ozone because of their different spectral weighting functions [15], T_{D} is the threshold exposure time for vitamin D synthesis, α is the fractional exposure area of skin, MEDF is the blocking factor relating to the minimal erythema dose (MED), which is estimated from the erythemal dose relating to the skin type, and SPF is the sun protection factor. Therefore, the MEDF is defined to be the number of standard erythemal doses (SED), which is corresponding to 100 J/m^2 for erythemal UV irradiance, for

given skin types. The DUVI is essentially a similar concept to estimate the UVI value, but it also considers the spectral difference due to the change in action spectra. Based on the DUVI value, the T_D is estimated to be

$$T_D = T_{D0} \times \left[\frac{10.0}{\text{UVI}}\right] \times \left[\frac{2.0}{R_{UV}}\right] \times \left[\frac{1}{\alpha}\right] \times \left[\frac{\text{MEDF}}{2.5}\right]. \quad (5)$$

The reference value of the exposure time (T_{D0}) corresponds to conditions under which the exposure time for vitamin D synthesis is 1 minute as described in previous studies [15, 69, 70]. If α and MEDF are assumed to be 0.1 and 4.5 (for Type IV skin), respectively, the equation for T_D simplifies to $T_D = 360.0/[R_{UV} \times \text{UVI}]$. The α for 0.1 is assumed to be from nominal cases of wintertime exposure skin surface area, with only the hands and face exposed. In some cases, the parameters related to the skin type and exposure of the skin surface area can have large variations. For example, high deficiencies of vitamin D were found in rural areas at high sun elevations in the equatorial region for dark skinned women [71]. In Youn et al. [72], the skin type of Korean mostly ranges from type III to V, and the skin type is related on the frequency of UV exposure and age. Although several factors related to the skin types can be considerable factor for accurate exposure time estimation, the factors of MEDF are applied the above assumed parameters (based on skin type IV) in this study.

Because the exposure time is estimated from the spectral UV irradiance with high spectral resolution, the R_{UV} can be directly estimated from the RTM results with simultaneous estimation of UV_{Ery} and UV_{VitD}. As the UV irradiance spectrum varies during the exposure time, the R_{UV} was defined as the average value during the exposure period. To calculate the T_D, based on the results, the UV irradiance from the RTM was interpolated with one-hour interval to a one-minute interval. After interpolation of the UV irradiance with a one-minute interval, T_D can be estimated with one-minute resolution.

3. Results and Validation

3.1. Annual and Seasonal Variation of UV. Figure 3 shows the simulated UV_{Ery} and UV_{VitD} before and after adopting the CMF, and, as shown in Table 1 for the six representative sites, the noon exposure time for vitamin D synthesis (T_D) and erythema dose (T_E). During the comparison period from January 2015 to September 2016, the T_D clearly shows a seasonal cycle, with the longest exposure times in winter (especially December) and the shortest in summer (May to July). Generally, the T_D follows the seasonal change in solar zenith angle. In summer, the minimum T_D was estimated to be less than 30 minutes. However, the simulated T_D was never less than 10 minutes. Although the cloud-free UV irradiance is highest in the summer season, the summertime UV_{VitD} is similar to that of the late spring and early autumn due to the high cloud cover due to the Asian monsoon season in summer.

During the winter, the T_D was generally longer than 100 minutes (December to February) and exceeded 200 minutes in December. Thus, sufficient synthesis is rarely possible by solar UV exposure alone during winter. The longest T_D was estimated during December, when the largest solar zenith angle occurred at noon on the winter solstice. In addition, the T_D variations were greater in the winter than in the summer. These variations were due to the low values of UV_{VitD} in the winter leading to reduced synthesis efficiency. For this reason, the day-to-day changes in T_D were largest in the winter, despite the small day-to-day changes in CMF.

Figure 4 shows the seasonal average of T_D at the representative sites at noon. During summer (June to August, JJA hereafter), the T_D was estimated to range from 12.35 to 14.10 minutes, while the T_D ranged from 50.97 to 99.62 minutes during the winter (December to February, DJF hereafter). The annual variation of T_D ranged from 38.62 (Gosan) to 85.52 minutes (Gangneung). Regardless of the season, the T_D was the longest in Gangneung and the shortest in Gosan and depended strongly on location, particularly latitude. The annual variation and seasonal average of T_D decreased from the north to the south. Compared with the T_D in spring (March to May, MAM hereafter) and autumn (September to November, SON hereafter), the six-site averaged T_D during MAM was 13 minutes shorter than that during SON. This is because the seasonal mean solar zenith angle during MAM was significantly smaller than that during SON. As shown in Figure 5, the overall characteristics of seasonal and annual variations of the T_D at 09:00 were similar to those at noon. The annual variation in T_D ranged from 98.86 (Gosan) to 153.49 minutes (Gangneung) and showed a strong latitudinal dependence. Furthermore, the six-site averaged T_D during MAM was 18 minutes shorter than that during SON, similar to the seasonal dependence seen at noon. The ratio of T_D at noon to that at 09:00 ranged from 1.90 (DJF at Gangneung) to 3.08 (MAM at Gosan). The variation of the T_D ratio at noon to 09:00 is related to differences in the solar zenith angle and the diurnal variations of the CMF. At all six stations, the diurnal variations of the T_D were smallest during the DJF and largest during the MAM.

3.2. Comparison and Error Analysis. To compare the simulation and observation of T_D and T_E, the broadband UV irradiance data from the UV biometer instruments at Seoul and Pohang are used. Because of differences in the observational periods and instrument maintenance, the comparison periods for the UV biometer were defined to be June 2015 to September 2016 in Seoul, and from January 2015 to September 2016 in Pohang. The UV biometer at Korean observation sites is designed to provide daily maximum UV values with uncertainties up to 5% [73]. However, the broadband instrument provides neither the spectral UV irradiance nor the UV_{VitD}. To estimate the UV_{VitD} and T_D from broadband observation, an alternative parameter for estimating R_{UV} is essential before the comparison. For this reason, an empirical approach was adopted to estimate R_{UV} from UVI alone to be able to adopt the UV_{VitD} estimation

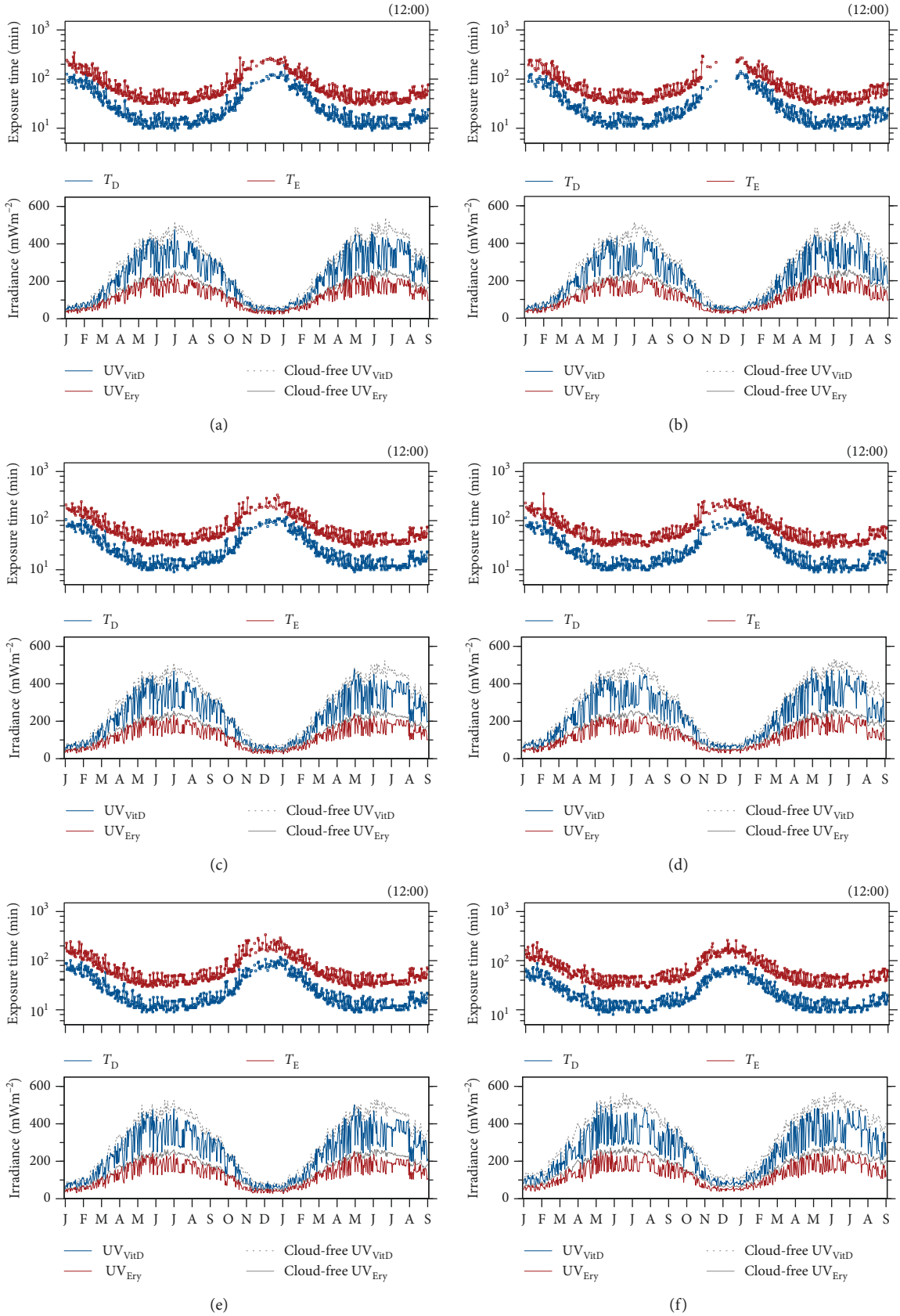

Figure 3: Time series of simulated UV irradiance and threshold exposure time for vitamin D synthesis and erythema dose at noon over (a) Seoul, (b) Gangneung, (c) Anmyeondo, (d) Pohang, (e) Mokpo, and (f) Gosan.

Table 1: List of representative region for the UV calculation.

Station	Latitude	Longitude	Altitude(m)	Urban index (UI)
Seoul	37.57	126.97	86	4
Gangneung	37.80	128.85	79	1
Anmyeondo	36.53	126.32	46	0
Pohang	36.03	129.38	2	0
Mokpo	34.82	126.38	38	2
Gosan	33.29	126.16	74	0

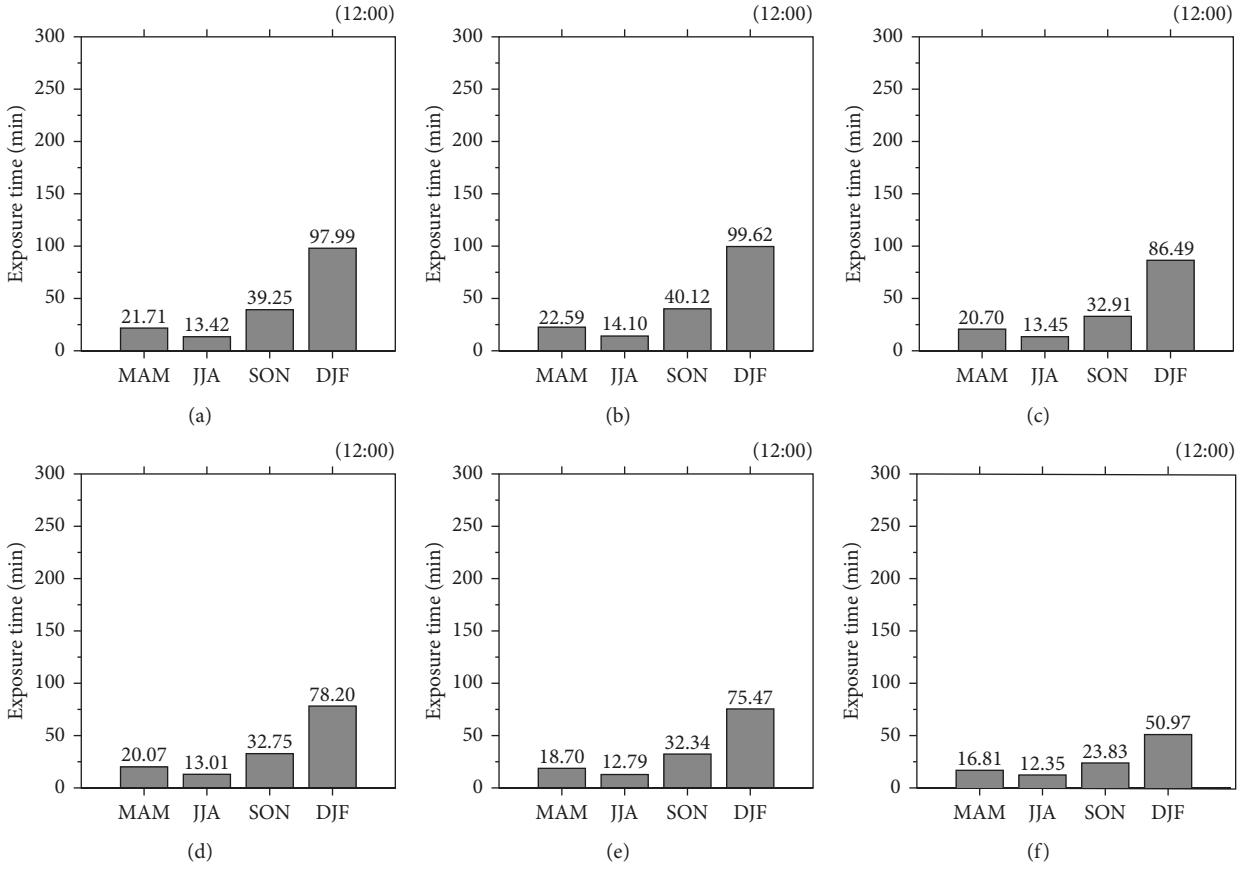

Figure 4: Seasonal average of threshold exposure time for vitamin D synthesis at 6 different stations at noon in (a) Seoul, (b) Gangneung, (c) Anmyeondo, (d) Pohang, (e) Mokpo, and (f) Gosan.

from the UV biometer. The empirical R_{UV} was estimated by applying a fit between the UVI and R_{UV} both derived from the spectral irradiance from the Brewer spectrophotometer in Seoul for cloud covers of less than two tenths for the period of 2006–2010. As shown in Figure 6, using this approach revealed a clear relationship in R_{UV} with UVI.

Figure 7 shows a scatter plot of the simulated and observed T_D at Seoul and Pohang. Due to the limitation of the empirical approaches for R_{UV}, the comparison was performed only for cloud-free days, which were defined as days during which the cloud covers from both observations and prediction from RDAPS was less than 2 (as the maximum value in 3-hour intervals). Overall, the number of data points selected for the comparison was 112 (09:00) and 91 (noon) for Seoul and 134 (09:00) and 112 (noon) for Pohang. In addition, Figure 7 represents the seasonal averaged T_D with its standard deviation as an error bar. Although the comparison was only performed under clear-sky conditions, the statistical result of the correlation coefficient of determination (R^2) ranged from 0.86 to 0.91. The mean biases of T_D between the observations and simulations ranged from −2.08 to 1.97 minutes, but compared to the bias values, the root mean square errors (RMSEs) at the two sites were relatively high. The RMSEs in Seoul were 21.70 minutes at 09:00 and 15.91 minutes at noon, and that in Pohang were 20.50 minutes at 09:00 and 9.36 minutes at noon.

However, the slope is always larger than 1.0. The slope at both 09:00 and noon is 1.6 in Seoul, and 1.2 and 1.3,

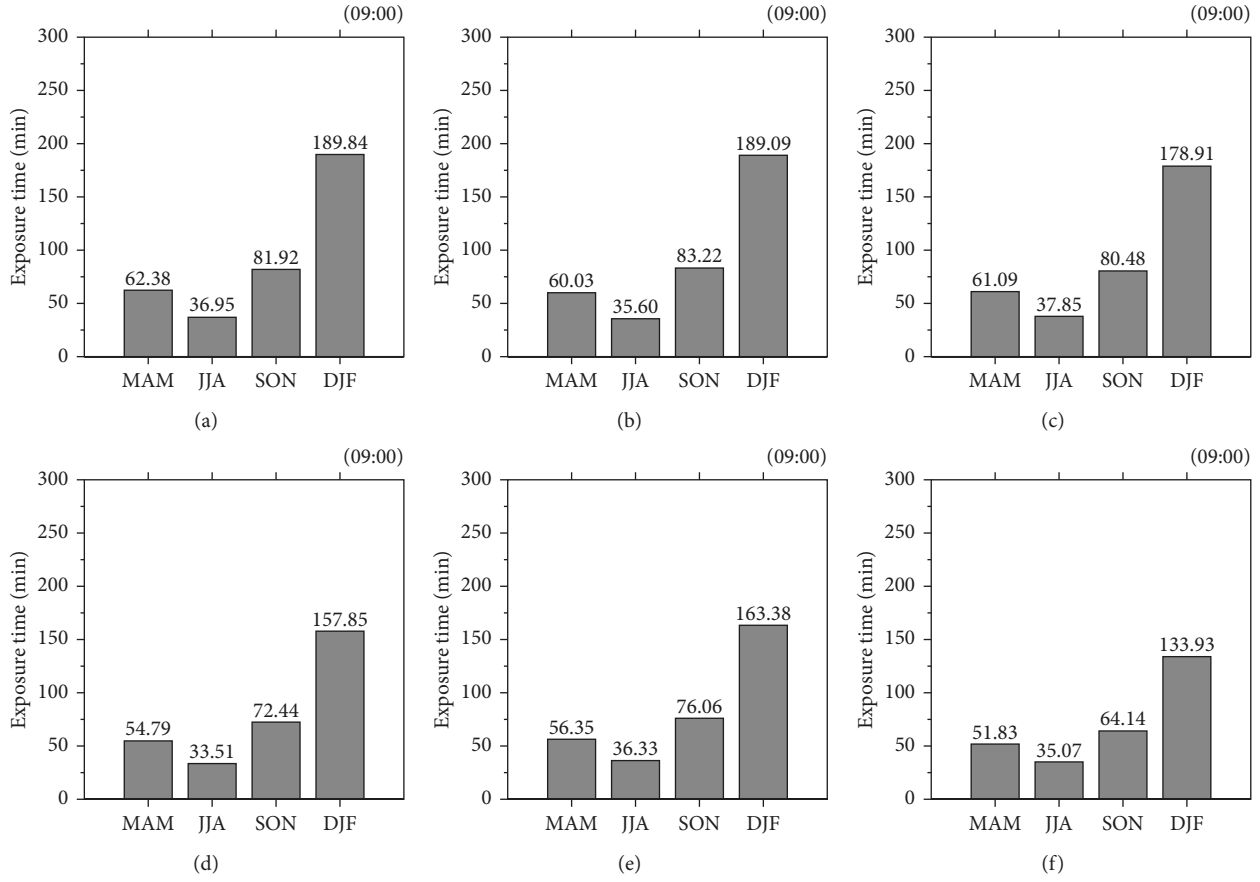

Figure 5: Seasonal average of threshold exposure time for vitamin D synthesis at 6 different stations at 9 a.m. in (a) Seoul, (b) Gangneung, (c) Anmyeondo, (d) Pohang, (e) Mokpo, and (f) Gosan.

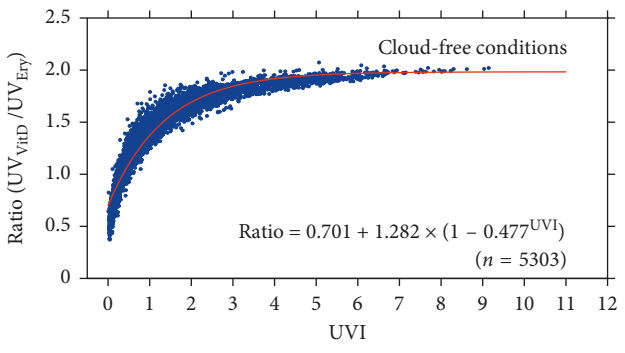

Figure 6: Relation between the R_{UV} and UVI from the hyperspectral observation of the Brewer spectrophotometer in Seoul (2006~2010) in clear-sky conditions.

respectively, in Pohang. In particular, the T_D differences increase under the condition for simulated $T_D > 150$ minutes. Because the exposure time for the synthesis is inversely related to the UV intensity, the T_D difference is enhanced under low UV irradiance conditions. Figure 8 shows the UVI value between the observation from UV biometer and the simulation under cloud-free conditions. In Figure 8, the slope between the observation and simulated UVIs ranges from 0.8 to 1.0. Furthermore, small negative biases are found for the simulated UVIs. The negative biases can affect the longer T_D values in the simulation, and the difference is greater under the cases with weak UV intensity. Therefore, the overestimation of T_D in the simulation is significant in cases where T_D is large.

Large RMSEs of T_D are thought to be from the error generated during the interpolation of the UV irradiance calculation and discrepancy of UV irradiance data between model and observation. T_D is calculated using all UV irradiance within the time during the exposure period. Because of the variations in cloud coverage and type, the real atmosphere causes dramatic changes in the surface irradiance. For this reason, the observed UV is fully evaluated to the atmospheric conditions with a one-minute resolution. Clearly, the observation data from the UV biometer also have interpolation process for exposure time estimation because of its temporal resolution of 10 minutes. However, the simulated UV irradiance at intervals of one minute is calculated by interpolating with the one-hour simulation. In particular, the predicted cloud amount for the CMF calculation is estimated in 3-hour intervals.

The UV attenuation by the cloud is a function of cloud cover, cloud types, and cloud optical thickness and its vertical distribution. However, the CMF in the simulation is simply fixed according to the cloud amount from the forecast model of KMA. Therefore, the simple calculation for

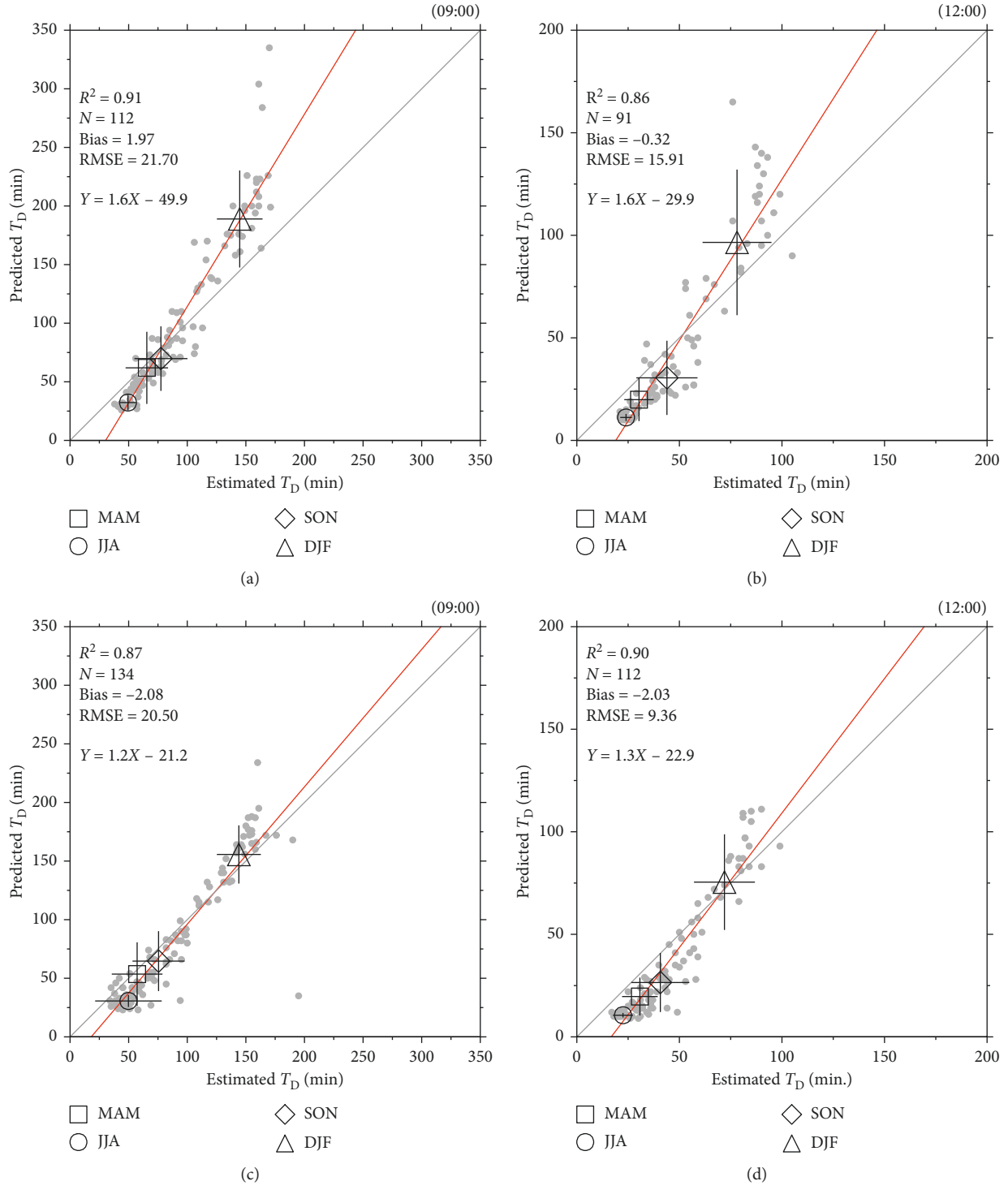

Figure 7: Scatter plot of threshold exposure time for vitamin D between the observation (Estimated T_D) and $(D+1)$ forecast simulation (Predicted T_D) based on cloud-free conditions in (a) Seoul at 9:00 (Korea Standard Time; KST) and (b) at 12:00 (KST) and in (c) Pohang at 9:00 (KST) and (d) at 12:00 (KST).

the CMF is one of error source in the T_D calculation. In addition, the attenuation due to real cloud conditions fluctuates, unlike the simulated cloud condition. Table 2 shows the CMF for the T_D simulation and the ratio of the UVI between the observed and clear-sky from the RTM, with respect to the cloud categories from the RDAPS. If the clear-sky UVI from the RTM is accurately defined to the atmospheric and surface conditions except for the clouds, the observed UVI over clear-sky UVI (CMF_{obs} hereafter) is assumed to be the effect of cloud attenuation, which is directly estimated for the CMF from the observation. For all the cloud categories, the standard deviation of CMF_{obs}

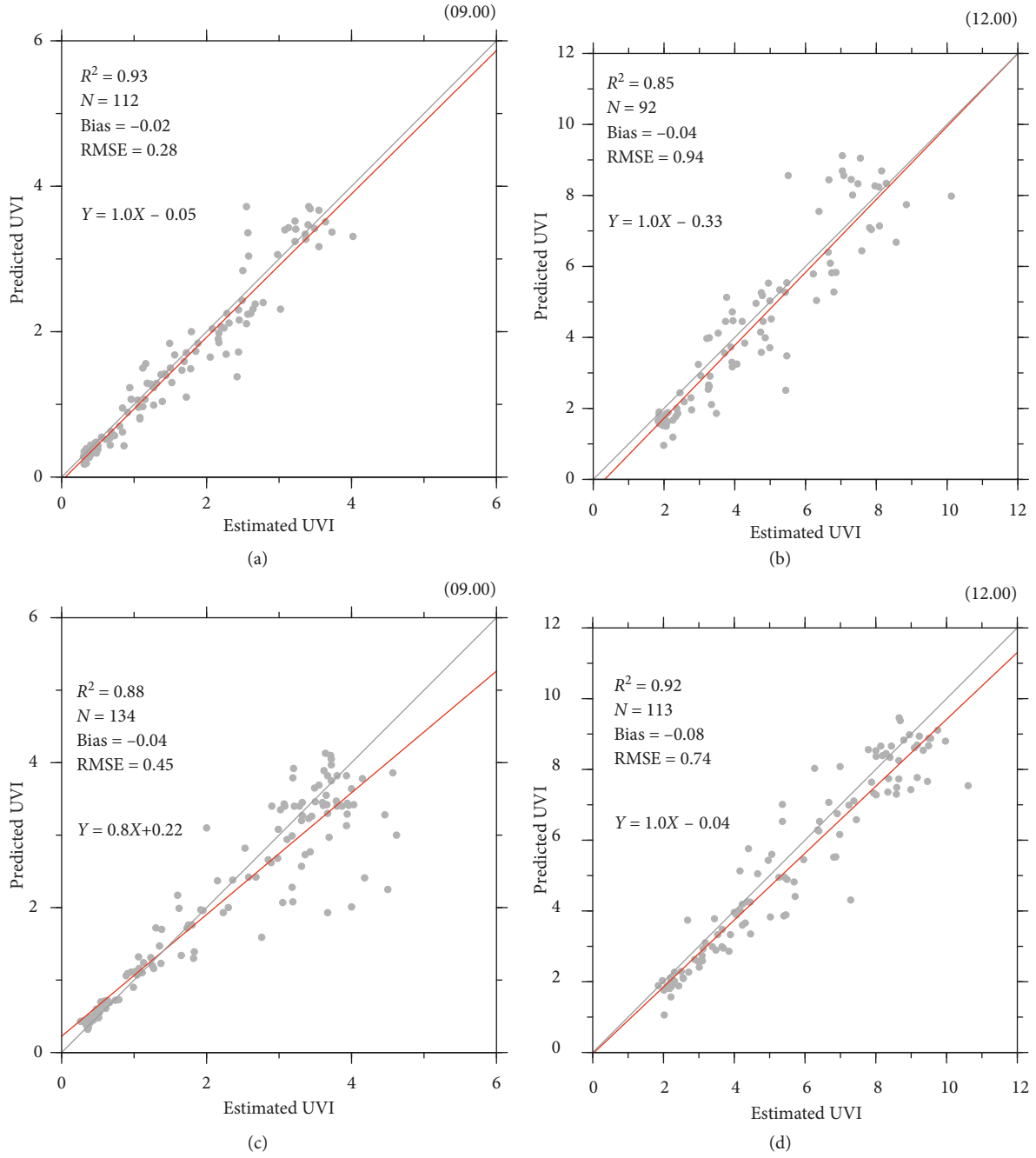

Figure 8: Scatter plot of UVI between the observation and simulation (Predicted UVI) based on cloud-free conditions in (a) Seoul at 9 a.m. and (b) at noon and in (c) Pohang at 9 a.m. and (d) at noon.

ranges from 0.162 to 0.225. In addition, the CMF_{obs} is more sensitive to the cloud amount than the CMF. For these reasons, the scatter plot of the UVI in Figure 8 shows large variations for most of the ranges of UVI, with a slight negative bias. In addition, the variation of T_D is larger in high T_D cases than that in small T_D cases, because the fitting curve for the R_{UV} from the observation varies greatly under low UVI conditions.

The predictions of total ozone are also thought to be an important source of errors in simulated T_D. Figure 9 shows a scatter plot between the predicted and observed total ozone for $(D+1)$ during the validation period. The correlation coefficients (R) were 0.86 and 0.84 at Seoul and Pohang, respectively, with an RMSE of approximately 22 DU. Moreover, there were high values for the mean absolute error (MAE) and mean absolute percentage error (MAPE), of approximately 16 DU and 5%, respectively. Previous study using data in Korea has shown that a 1% change in total ozone resulted in a 1.0%–1.2% change in surface erythemal UV irradiance [74]. The amplitude of the UV irradiance change due to the total ozone variation in Korea is similar to those from other model studies [75, 76]. Therefore,

Table 2: Mean and standard deviation of CMF_{obs} with respect to the cloud categories from the numerical weather prediction results.

Cloud categories	Cloud amount	CMF_{obs}		CMF
		Seoul	Pohang	
No clouds	0~2	0.812 (±0.177)	0.859 (±0.196)	0.984
Partly cloudy 1	3~5	0.748 (±0.186)	0.828 (±0.194)	0.918
Partly cloudy 2	6~7	0.652 (±0.186)	0.765 (±0.225)	0.784
Overcast 1	8~9	0.501 (±0.191)	0.570 (±0.221)	0.579
Overcast 2	10	0.267 (±0.162)	0.307 (±0.185)	0.450

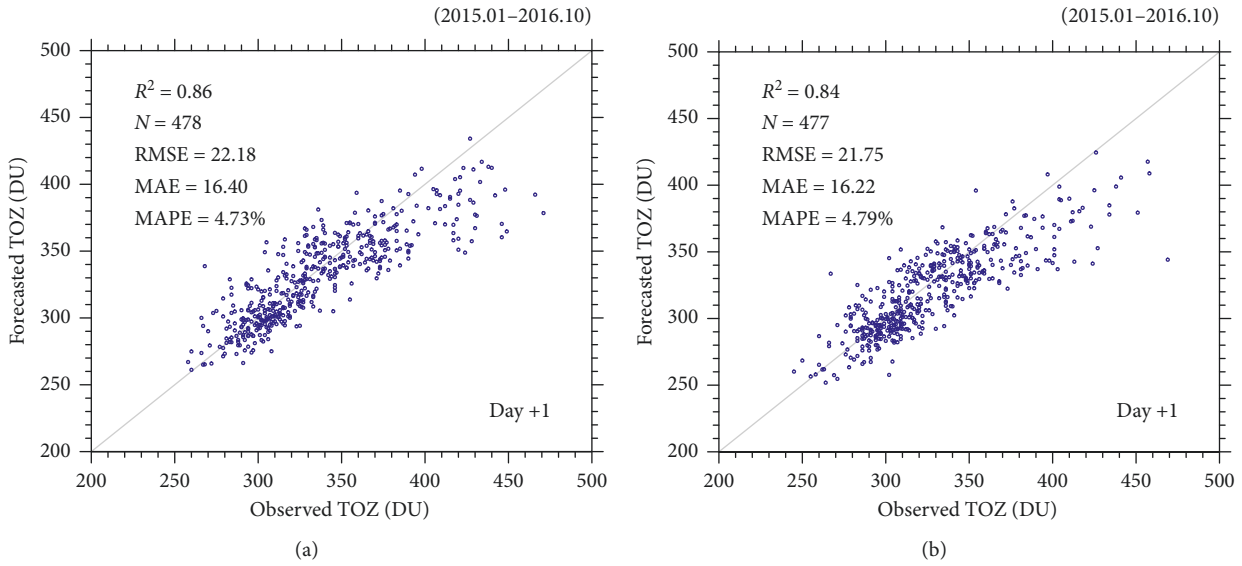

Figure 9: Scatter plot of total ozone between the observed and forecasted values in (a) Seoul and (b) Pohang.

the RMSE of 22 DU corresponds to an approximate 7%-8% variation in UV. In addition, the T_D variation was more sensitive to the variation in UV irradiance during the winter than the other seasons. Figure 10 shows the seasonal RMSE of total ozone between observations and predictions. The RMSE was larger during DJF and MAM than during JJA and SON, which had the weakest UV irradiance. Therefore, the seasonal dependence of errors in the prediction of total ozone partially accounted for the large discrepancy in the simulated T_D.

In the UV model simulation, the AOD value is assumed to be same in time and space. However, spatiotemporal distribution of aerosol is highly varied in the real atmosphere. Figure 11 shows the time series of daily AOD at 550 nm (AOD_{550} hereafter) in South Korea by using the Level 2 Aerosol product from Moderate Resolution Imaging Spectroradiometer (MODIS) (MYD04 hereafter) in the year 2016. We assumed to be the South Korea region as a grid box of 33.0~38.6°N and 124.5~131.0°E. To estimate the AOD_{550} from MODIS in South Korea, we selected the pixels with the quality flag as "good" and "very good." Yearly averaged AOD_{550} is 0.31 with temporal standard deviation of 0.17. For the spatial variation of AOD_{550}, we also estimated to the spatial standard deviation of AOD_{550} in South Korea, and yearly averaged spatial standard deviation is 0.17. Based on the yearly averaged AOD_{550}, relative variation is 44.2% and 54.6% for spatial and temporal variation, respectively. From Kim et al. [23], relative difference of erythemal UV irradiance by changing 1% of AOD was estimated to be 0.29 ± 0.06% from the observation in Seoul. Although the spectral definition of AOD is different between MODIS and model simulation, the UV simulation error is estimated to be 12.8% and 15.8% for spatial and temporal variation of AOD, respectively, based on the sensitivity study of Kim et al. [23].

4. Conclusion and Discussion

In this study, the T_D was estimated over South Korea using simulated UV radiation from RTM. To calculate the spectral UV irradiance from RTM, a statistical linear regression method was applied to predict total ozone amount for one-day forecasts. Satellite observations of total ozone and its climatology were used to capture the general variability of total ozone. Wind, temperature, and geopotential height from the upper troposphere to the lower stratosphere were used to estimate the short-term variability of the total ozone due to atmospheric dynamics. In addition, particularly in urban areas, surface albedo variations were assumed to be dependent on the land-cover type. Using satellite measurements, the surface albedo was classified according to land-cover type and applied to the observational sites. After

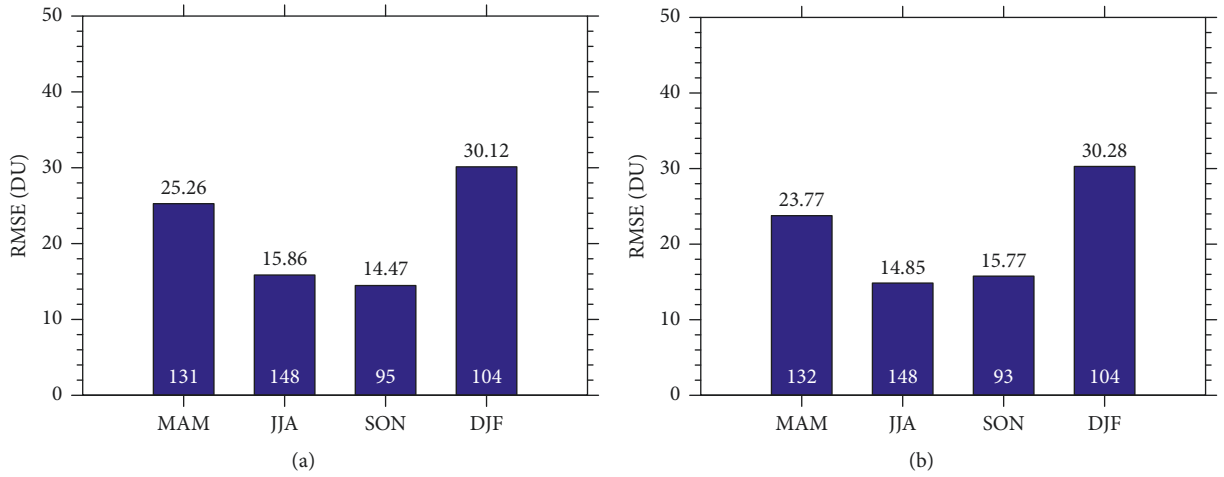

Figure 10: Seasonal characteristics of total ozone RMSE between the observed and forecasted value ($D+1$) in (a) Seoul and (b) Pohang.

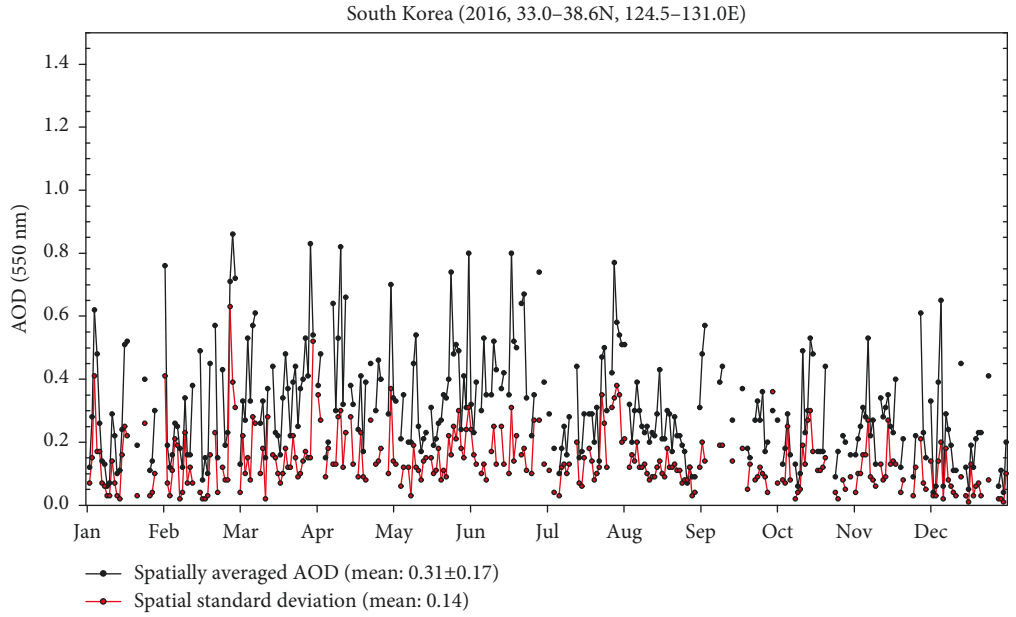

Figure 11: Time series of daily averaged and spatial standard deviation of AOD_{550} in South Korea (year 2016).

these applications to surface albedo and the prediction of total ozone, an RTM was used to estimate the clear-sky UV radiation.

A CMF was applied after calculating the clear-sky UV_{Ery}, because of the difficulty in converting cloud amount to optical depth for use in the one-dimensional RTM. The CMF was calculated as a function of cloud amount applied to the forecast results of the RDAPS from the KMA. Finally, the simulated UV irradiance dataset was interpolated from a one-hour to a one-minute resolution, and the T_D was estimated after considering the diurnal changes of spectral UV irradiance with high temporal resolution. Because of this high temporal resolution, the seasonal cycle and diurnal variations of T_D can be determined. In addition, local weather conditions were accounted for the T_D calculation by considering the cloud attenuation.

A comparison of modeled T_D with data from UVI observation sites revealed that the simulated T_D values had small biases with large deviations. In addition, the differences in T_D between the simulated and observed values are greater under weak UV irradiance conditions. T_D discrepancies between the observations and simulations were caused by UV estimation errors due to simple interpolation for UV estimation from the one-hour to one-minute interval and the simple CMF assumption. The simulation error for the prediction of total ozone also affected the deviations of the T_D. The 22 DU RMSE for the predicted total ozone arose from short-term variations. Because of the large short-term discrepancies of the total ozone, the modeled UV irradiance varied from 7% to 8%. In addition, the modeled UV irradiance also varied between 12.8% and 15.8% due to the spatial and temporal variation of AOD in South Korea,

respectively. From this validation study and error analysis, it is evident that more accurate regression methods for the prediction of total ozone, modification factors for cloud attenuation, and considering seasonal variations of aerosol are required to improve the accuracy of the simulation of T_D.

Data Availability

The total ozone data from OMI, surface type data from MODIS, RDAPS model, and UV observation data from KMA were used. Brief descriptions of the data are explained in the manuscript in Section 2. (1) The Level 3 data of total ozone from OMI is provided in the Mirador Earth Science Search in NASA. (2) The surface type data named MCD12C1 is provided in the site of USGS (https://lpdaac.usgs.gov). (3) The RDAPS of the UM from the KMA are used after confirming from the Korean Meteorological Administration. (4) The UV observation data from KMA also used after confirming from the Korean Meteorological Administration.

Conflicts of Interest

The authors declare that they have no conflicts of interest.

Acknowledgments

This study was supported by the Korea Meteorological Administration Research and Development Program under grant KMIPA 2015–5170 and the National Institutes of Environmental Research (NIER) funded by the Ministry of Environment (MOE) of the Republic of Korea (grant number NIER-2018-01-01-020).

References

[1] B. L. Diffey, "Ultraviolet radiation physics and the skin," *Physics in Medicine and Biology*, vol. 25, no. 3, pp. 405–426, 2000.

[2] B. L. Diffey, "Solar ultraviolet radiation effects on biological systems," *Physics in Medicine and Biology*, vol. 36, no. 3, pp. 299–328, 1981.

[3] M. M. Caldwell, L. O. Björn, J. F. Bornman et al., "Effects of increased solar ultraviolet radiation on terrestrial ecosystems," *Journal of Photochemistry and Photobiology B: Biology*, vol. 46, no. 1-3, pp. 40–52, 1998.

[4] S. Madronich, R. L. McKenzie, L. O. Björn, and M. M. Caldwell, "Changes in biologically active ultraviolet radiation reaching the Earth's surface," *Journal of Photochemistry and Photobiology B: Biology*, vol. 46, no. 1–3, pp. 5–19, 1998.

[5] A. F. McKinlay and B. L. Diffey, "A reference action spectrum for ultraviolet induced erythema in human skin," in *Human Exposure to Ultraviolet Radiation: Risks and Regulations*, W. R. Passchler and B. F. M. Bosnajakovic, Eds., pp. 83–87, 1987.

[6] R. B. Setlow, "The wavelengths in sunlight effective in producing skin cancer: a theoretical analysis," *Proceedings of the National Academy of Sciences*, vol. 71, no. 9, pp. 3363–3366, 1974.

[7] S. S. Park, Y. G. Lee, and J. H. Kim, "Impact of UV-A radiation on erythemal UV and UV-index estimation over Korea," *Advances in Atmospheric Sciences*, vol. 32, no. 12, pp. 1639–1646, 2015.

[8] A. Juzeniene and J. Moan, "Beneficial effects of UV radiation other than via vitamin D production," *Dermato-Endocrinology*, vol. 4, no. 2, pp. 109–117, 2014.

[9] R. K. Sivamani, L. A. Crane, and R. P. Dellavalle, "The benefits and risks of Ultraviolet Tanning and its alternatives: the role of prudent Sun exposure," *Dermatologic Clinics*, vol. 27, no. 2, pp. 149–154, 2009.

[10] M. R. Albert and K. G. Ostheimer, "The evolution of current medical and popular attitudes toward ultraviolet light exposure: Part 1," *Journal of the American Academy of Dermatology*, vol. 47, no. 6, pp. 930–937, 2002.

[11] M. R. Albert and K. G. Ostheimer, "The evolution of current medical and popular attitudes toward ultraviolet light exposure: Part 2," *Journal of the American Academy of Dermatology*, vol. 48, no. 6, pp. 909–918, 2003.

[12] M. R. Albert and K. G. Ostheimer, "The evolution of current medical and popular attitudes toward ultraviolet light exposure: part 3," *Journal of the American Academy of Dermatology*, vol. 49, pp. 1096–1106, 2003.

[13] M. F. Holick, "Environmental factors that influence the cutaneous production of vitamin D," *The American Journal of Clinical Nutrition*, vol. 61, no. 3, pp. 638S–645S, 1995.

[14] D. Wolpowitz and B. A. Gilchrest, "The vitamin D questions: how much do you need and how should you get it?," *Journal of the American Academy of Dermatology*, vol. 54, no. 2, pp. 301–317, 2006.

[15] R. L. McKenzie, J. B. Liley, and L. O. Björn, "UV radiation: balancing risks and benefits," *Photochemistry and Photobiology*, vol. 85, no. 1, pp. 88–98, 2009.

[16] CIE (International Commission on Illumination), *Action Spectrum from the Production of Previtamin D3 in Human Skin, Publication No. CIE 174*, CIE (International Commission on Illumination), Vienna, Austria, 2006.

[17] M. G. Kimlin, "Geographic location and vitamin D synthesis," *Molecular Aspects of Medicine*, vol. 29, no. 6, pp. 453–461, 2008.

[18] M. K. B. Bogh, "Vitamin D production after UVB: aspects of UV-related and personal factors," *Scandinavian Journal of Clinical and Laboratory Investigation-Supplement*, vol. 72, pp. 24–31, 2012.

[19] J. MacLaughlin, R. Anderson, and M. Holick, "Spectral character of sunlight modulates photosynthesis of previtamin D3 and its photoisomers in human skin," *Science*, vol. 216, no. 4549, pp. 1001–1003, 1982.

[20] A. R. Webb and O. Engelsen, "Calculated Ultraviolet exposure levels for a healthy vitamin D status," *Photochemistry and Photobiology*, vol. 82, no. 6, pp. 1697–1703, 2006.

[21] J. E. Fredrick, H. E. Snell, and E. K. Haywood, "Solar ultraviolet radiation at the Earth's surface," *Photochemistry and Photobiology*, vol. 50, pp. 443–450, 1989.

[22] J. Bilbao, R. Román, C. Yousif, D. Mateos, and A. de Miguel, "Total ozone column, water vapour and aerosol effects on erythemal and global solar irradiance in Marsaxlokk, Malta," *Atmospheric Environment*, vol. 99, pp. 508–518, 2014.

[23] J. Kim, H.-K. Cho, J. Mok, H. D. Yoo, and N. Cho, "Effects of ozone and aerosol on surface UV radiation variability," *Journal of Photochemistry and Photobiology B: Biology*, vol. 119, pp. 46–51, 2013.

[24] M. Antón, A. Serrano, M. L. Cancillo, and J. A. García, "An empirical model to estimate ultraviolet erythemal transmissivity," *Annales Geophysicae*, vol. 27, no. 4, pp. 1387–1398, 2009.

[25] J. Calbo, D. Pages, and J. A. Gonzalez, "Empirical studies of cloud effects on UV radiation: a review," *Reviews of Geophysics*, vol. 43, no. 2, 2005.

[26] Y. G. Lee, J.-H. Koo, and J. Kim, "Influence of cloud fraction and snow cover to the variation of surface UV radiation at King Sejong station, Antarctica," *Atmospheric Research*, vol. 164-165, pp. 99–109, 2015.

[27] O. Engelsen, M. Brustad, L. Aksnes, and E. Lund, "Daily duration of vitamin D synthesis in human skin with relation to latitude, total ozone, altitude, ground cover, aerosols, and cloud thickness," *Photochemistry and Photobiology*, vol. 81, no. 6, pp. 1287–1290, 2007.

[28] A. R. Webb, L. Kline, and M. F. Holick, "Influence of season and latitude on the cutaneous synthesis of vitamin D3: exposure to winter sunlight in Boston and Edmonton will not promote vitamin D3Synthesis in human skin∗," *Journal of Clinical Endocrinology and Metabolism*, vol. 67, no. 2, pp. 373–378, 1988.

[29] V. E. Fioletov, L. J. B. McArthur, T. W. Mathews, and L. Marrett, "Estimated ultraviolet exposure levels for a sufficient vitamin D status in North America," *Journal of Photochemistry and Photobiology B: Biology*, vol. 100, no. 2, pp. 57–66, 2010.

[30] M. Miyauchi, C. Hirai, and H. Nakajima, "The solar exposure time required for Vitamin D3 synthesis in the Human body estimated by Numerical simulation and observation in Japan," *Journal of Nutritional Science and Vitaminology*, vol. 59, no. 4, pp. 257–263, 2013.

[31] Y. G. Lee, J. Kim, H.-K. Cho, and C. H. Song, "Regional forecast of the UV index with optimized total ozone prediction using satellite observations over East Asia," *International Journal of Remote Sensing*, vol. 30, no. 22, pp. 6035–6051, 2009.

[32] W. R. Burrows, M. Vallee, D. I. Wardle, J. B. Kerr, L. J. Wilson, and D. W. Tarasick, "The Canadian operational procedure for forecasting total ozone and UV radiation," *Meteorological Applications*, vol. 1, no. 3, pp. 247–265, 2007.

[33] U. Feister, G. Laschewski, and R.-D. Grewe, "UV index forecasts and measurements of health-effective radiation," *Journal of Photochemistry and Photobiology B: Biology*, vol. 102, no. 1, pp. 55–68, 2011.

[34] P. Gies, C. Roy, J. Javorniczky, S. Henderson, L. Lemus-Deschamps, and C. Driscoll, "Global solar UV index: Australian measurements, forecasts and comparison with the UK¶," *Photochemistry and Photobiology*, vol. 79, no. 1, pp. 32–39, 2011.

[35] J. W. Krzyscin, J. Jaroslawski, and P. Sobolewski, "On an improvement of UV index forecast: UV index diagnosis and forecast for Belsk, Poland, in Spring/Summer 1999," *Journal of Atmospheric and Solar-Terrestrial Physics*, vol. 63, no. 15, pp. 1593–1600, 2001.

[36] C. S. Long, A. J. Miller, H.-T. Lee, J. D. Wild, R. C. Przywarty, and D. Hufford, "Ultraviolet index forecasts issued by the National weather service," *Bulletin of the American Meteorological Society*, vol. 77, no. 4, pp. 729–748, 1996.

[37] A. W. Schmalwieser and G. Schauberger, "Validation of the Austrian forecast model for solar, biologically effective UV radiation-UV index for Vienna," *Journal of Geophysical Research: Atmospheres*, vol. 105, no. D21, pp. 26661–26667, 2000.

[38] C. S. Zerefos, K. Tourpali, K. Eleftheratos et al., "Evidence of a possible turning point in solar UV-B over Canada, Europe and Japan," *Atmospheric Chemistry and Physics*, vol. 12, no. 5, pp. 2469–2477, 2012.

[39] T. T. Sekiyama and K. Shibata, "Predictability of total ozone using a global three-dimensional chemical transport model coupled with the MRI/JMA98 GCM," *Monthly Weather Review*, vol. 133, no. 8, pp. 2262–2274, 2005.

[40] Y. K. Kim, H. W. Lee, J. K. Park, and Y. S. Moon, "The stratosphere-troposphere exchange of ozone and aerosols over Korea," *Atmospheric Environment*, vol. 36, no. 3, pp. 449–463, 2002.

[41] S. S. Park, J. Kim, H. K. Cho, H. Lee, Y. Lee, and K. Miyagawa, "Sudden Increase in the total ozone density due to secondary ozone peaks and its effect on total ozone trends over Korea," *Atmospheric Environment*, vol. 47, pp. 226–235, 2012.

[42] S. S. Park, J. Kim, N. Cho, Y. G. Lee, and H. K. Cho, "The variations of stratospheric ozone over the Korean Peninsula 1985~2009," *Atmosphere-KMS*, vol. 21, no. 4, pp. 349–359, 2011.

[43] H. K. Cho, M. J. Jeong, J. Kim, and Y. J. Kim, "Dependence of diffuse photosynthetically active solar irradiance on total optical depth," *Journal of Geophysical Research: Atmospheres*, vol. 108, no. D9, p. 4267, 2003.

[44] V. E. Fioletov, J. B. Kerr, E. W. Hare, G. J. Labow, and R. D. McPeters, "An assessment of the world ground-based total ozone network performance from the comparison with satellite data," *Journal of Geophysical Research: Atmospheres*, vol. 104, no. D1, pp. 1737–1747, 1999.

[45] R. D. McPeters and G. J. Labow, "An assessment of the accuracy of 14.5 years of Nimbus 7 TOMS version 7 ozone data by comparison with the Dobson network," *Geophysical Research Letters*, vol. 23, no. 25, pp. 3695–3698, 1996.

[46] D. Balis, M. Kroon, M. E. Koukouli et al., "Validation of Ozone Monitoring Instrument total ozone column measurements using Brewer and Dobson spectrophotometer ground-based observations," *Journal of Geophysical Research*, vol. 112, no. D24, 2007.

[47] J. Kim, J. Kim, H.-K. Cho et al., "Intercomparison of total column ozone data from the Pandora spectrophotometer with Dobson, Brewer, and OMI measurements over Seoul, Korea," *Atmospheric Measurement Techniques*, vol. 10, no. 10, pp. 3661–3676, 2017.

[48] I. Foyo-Moreno, I. Alados, F. J. Olmo, and L. Alados-Arboledas, "The influence of cloudiness on UV global irradiance (295-385 nm)," *Agricultural and Forest Meteorology*, vol. 120, no. 1–4, pp. 101–111, 2003.

[49] D. Mateos, A. di Sarra, J. Bilbao et al., "Spectral attenuation of global and diffuse UV irradiance and actinic flux by clouds," *Quarterly Journal of the Royal Meteorological Society*, vol. 141, no. 686, pp. 109–113, 2014.

[50] D. M. Villan, A. de Miguel Castrillo, and J. B. Santos, "Empirical models of UV total radiation and cloud effect study," *International Journal of Climatology*, vol. 30, pp. 1407–1415, 2010.

[51] A. F. Bais, C. S. Zerefos, and C. T. McElroy, "Solar UVB measurements with the double- and single-monochromator Brewer ozone spectrophotometers," *Geophysical Research Letters*, vol. 23, no. 8, pp. 833–836, 1996.

[52] S. Thiel, K. Steiner, and H. K. Seidlitz, "Modification of global erythemally effective irradiance by clouds," *Photochemistry and Photobiology*, vol. 65, no. 6, pp. 969–973, 1997.

[53] J. Sabburg and J. Wong, "The effect of clouds on enhancing UVB irradiance at the Earth's surface: a one year study," *Geophysical Research Letters*, vol. 27, no. 20, pp. 3337–3340, 2000.

[54] J. M. Sabburg, A. V. Parisi, and M. G. Kimlin, "Enhanced spectral UV irradiance: a 1 year preliminary study," *Atmospheric Research*, vol. 66, no. 4, pp. 261–272, 2003.

[55] J. S. Schafer, V. K. Saxena, B. N. Wenny, W. Barnard, and J. J. De Luisi, "Observed influence of clouds on ultraviolet-B radiation," *Geophysical Research Letters*, vol. 23, no. 19, pp. 2625–2628, 1996.

[56] A. Lindfors and A. Arola, "On the wavelength-dependent attenuation of UV radiation by clouds," *Geophysical Research Letters*, vol. 35, no. 5, article L05806, 2008.

[57] J. M. Sabburg and A. V. Parisi, "Spectral dependency of cloud enhanced UV irradiance," *Atmospheric Research*, vol. 81, no. 3, pp. 206–214, 2006.

[58] G. Seckmeyer, R. Erb, and A. Albold, "Transmittance of a cloud is wavelength-dependent in the UV-range," *Geophysical Research Letters*, vol. 23, no. 20, pp. 2753–2755, 1996.

[59] J. W. Krzyścin, J. Jarosławski, and P. S. Sobolewski, "Effects of clouds on the surface erythemal UV-B irradiance at northern midlatitudes: estimation from the observations taken at Belsk, Poland (1999–2001)," *Journal of Atmospheric and Solar-Terrestrial Physics*, vol. 65, no. 4, pp. 457–467, 2003.

[60] M. E.-N. Adam and S. M. El Shazly, "Attenuation of UV-B radiation in the atmosphere: clouds effect, at Qena (Egypt)," *Atmospheric Environment*, vol. 41, no. 23, pp. 4856–4864, 2007.

[61] R. H. Grant and G. M. Heisler, "Estimation of ultraviolet-B irradiance under variable cloud conditions," *Journal of Applied Meteorology*, vol. 39, no. 6, pp. 904–916, 2000.

[62] S. Trepte and P. Winkler, "Reconstruction of erythemal UV irradiance and dose at Hohenpeissenberg (1968?2001) considering trends of total ozone, cloudiness and turbidity," *Theoretical and Applied Climatology*, vol. 77, no. 3-4, pp. 159–171, 2004.

[63] S. S. Park, M. Kim, H. Lee, H. Lee, S.-M. Kim, and Y. G. Lee, "Estimating cloud and aerosol UV modification factors based on spectral measurement from the Brewer spectrophotometer," *Atmosphere*, vol. 8, no. 6, pp. 109–126, 2017.

[64] S. Madronich, "UV radiation in the natural and perturbed atmosphere," in *UV-B Radiation and Ozone Depletion. Effects on Humans, Animals, Plants, Microorganisms and Materials*, M. Tevini, Ed., pp. 17–69, 1993.

[65] J. J. Michalsky and P. W. Kiedron, "Comparison of UV-RSS spectral measurements and TUV model runs for clear skies for the May 2003 ARM aerosol intensive observation period," *Atmospheric Chemistry and Physics*, vol. 8, no. 6, pp. 1813–1821, 2008.

[66] J. –H. Koo, J. Kim, M. Kim, H.-K. Cho, K. Aoki, and M. Yamano, "Analysis of aerosol optical properties in Seoul using skyradiometer observation," *Atmosphere-KMS*, vol. 17, pp. 407–420, 2007.

[67] U. Feister and R. Grewe, "Spectral albedo measurements in the UV and visible region over different types of surfaces," *Photochemistry and Photobiology*, vol. 62, no. 4, pp. 136–144, 1995.

[68] A. V. Parisi, J. Sabburg, M. G. Kimlin, and N. Downs, "Measured and modelled contributions to UV exposures by the albedo of surfaces in an urban environment," *Theoretical and Applied Climatology*, vol. 76, no. 3-4, pp. 181–188, 2003.

[69] M. F. Holick, "Vitamin D: the underappreciated D-lightful hormone that is important for skeletal and cellular health," *Current Opinion in Endocrinology and Diabetes*, vol. 9, no. 1, pp. 87–98, 2002.

[70] M. F. Holick, "Vitamin D deficiency," *New England Journal of Medicine*, vol. 357, no. 3, pp. 266–281, 2007.

[71] T. Gebreegziabher and B. J. Stoecker, "Vitamin D insufficiency in a sunshine-sufficient area: Southern Ethiopia," *Food and Nutrition Bulletin*, vol. 34, no. 4, pp. 429–433, 2013.

[72] J.-I. Youn, Y.-B. Choe, S. –B. Park et al., "The Fitzpatrick skin type in Korean People," *Korean Journal of Dermatology*, vol. 38, no. 7, pp. 920–927, 2000.

[73] Solar light Co., *501 UV Biometer Owners Manual*, Solar Light Co., Glenside, PA, USA, 2006.

[74] W. Kim, J. Kim, S. S. Park, and H.-K. Cho, "UV sensitivity to changes in Ozone, Aerosols, and clouds in Seoul, South Korea," *Journal of Applied Meteorology and Climatology*, vol. 53, no. 2, pp. 310–322, 2014.

[75] M. I. Hegglin and T. G. Shepherd, "Large climate-induced changes in ultraviolet index and stratosphere-to-troposphere ozone flux," *Nature Geoscience*, vol. 2, no. 10, pp. 687–691, 2009.

[76] S. Madronich, "Analytic formula for the clear-sky UV index," *Photochemistry and Photobiology*, vol. 83, no. 6, pp. 1537-1538, 2007.